JASS *Journal of Astronomy and Space Sciences*

Diagnostics of Diffuse Two-Phase Matter Using Techniques of Positron Annihilation Spectroscopy in Gamma-Ray and Optical Spectra

Dmytry Doikov[1], Alexander Yushchenko[2], Yeuncheol Jeong[3†]

[1]Department of Mathematics, Physics and Astronomy, Odessa National Maritime University, Odessa 65029, Ukraine
[2]Astrocamp Contents Research Institute, Goyang 10329, Korea
[3]Daeyang Humanity College, Sejong University, Seoul 05006, Korea

This paper is a part of the series on positron annihilation spectroscopy of two-phase diffuse gas-and-dust aggregates, such as interstellar medium and the young remnants of type II supernovae. The results obtained from prior studies were applied here to detect the relationship between the processes of the annihilation of the K-shell electrons and incident positrons, and the effects of these processes on the optical spectra of their respective atoms. Particular attention was paid to the Doppler broadening of their optical lines. The relationship between the atomic mass of the elements and the Doppler broadening, $\Delta\lambda_D$ (Å), of their emission lines as produced in these processes was established. This relationship is also illustrated for isotope sets of light elements, namely $_2^3$He, $_3^6$Li, $_3^7$Li, $_4^7$Be, $_4^9$Be, $_5^{10}$B, and $_5^{11}$B. A direct correlation between the γ-line luminosity (E_γ=1.022 MeV) and $\Delta\lambda_D$ (Å) was proved virtually. Qualitative estimates of the structure of such lines depending on the positron velocity distribution function, f(E), were made. The results are presented in tabular form and can be used to set up the objectives of further studies on active galactic nuclei and young remnants of type II supernovae.

Keywords: astroparticle physics, nuclear reactions, galaxies: active, galaxies: nuclei, gamma-rays: galaxies

1. INTRODUCTION

High luminosity (L_g) of active galactic nuclei (AGN) enables us to study distant galaxies. Often, the luminosity (L_g) is so high that the condition $L_g \gg L_s$, can be used, where L_s is the luminosity of the entire stellar population in a galaxy under study. In our earlier papers (Doikov 2018; Doikov et al. 2019), we have shown that such high luminosities can be associated with a high density of hard quanta and high-energy particle fluxes throughout the entire bulk of the AGN.

Energy losses due to ionization along the disc component, caused by such fluxes, result in the creation of predominant K-vacancies. Quanta resulting from stimulated emissions from cascade transitions to vacant atomic K energy levels span the spectral regions from soft X-ray to optical bands. Furthermore, optical and ultraviolet quanta, as well as non-thermal electrons, induce IR and radio emissions as shown by Doikov et al. (2018). Therefore, under similar physical conditions, one should expect that particles accelerated by the central compact object—that is, protons, α-particles, electrons, and positrons—will interact with a relatively stationary component of the AGN. Spallation reactions serve as indicators of such processes.

Fan et al. (2016) and Moskalenko & Strong (1998) investigated the overabundance of light elements in the circumcenter regions of galaxies and ascribed it to spallation reactions (Crosas & Weisheit 1996) associated with the proton component of cosmic rays within the AGN. Proton-rich nuclei produced in spallation reactions act as sources of positrons. Under such conditions, the reactions between protons, and less often those between α-particles and interstellar hydrogen atoms, can be considered to be the second source of positrons.

When the energies of protons and, in some cases, those of α-particles are approximately 2 GeV, a so-called state of Δ-resonance is reached as pointed out before by Dermer (1984, 1986) and Moskalenko & Strong (1998). It leads to the following cascades of particles:

$$p+H \rightarrow \pi^+ + \cdots; \ \pi^+ \rightarrow \mu^+ + \cdots; \ \mu^+ \rightarrow e^+ + \cdots$$
$$p+H \rightarrow \pi^- + \cdots; \ \pi^- \rightarrow \mu^- + \cdots; \ \mu^- \rightarrow e^- + \cdots \quad (1)$$
$$p+H \rightarrow \pi^0 + \cdots; \ \pi^0 \rightarrow 2\gamma$$
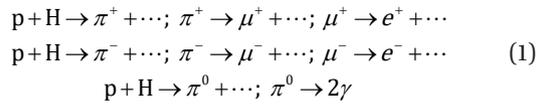
Gamma-quanta with energy equal to 67.5 MeV are represented by the third chain in cascades; they are described by equation (1) and can serve as indicators of such reactions. Cascades (Eq. 1) also illustrate alternative three-step patterns, resulting in the creation of electrons and positrons. Positron annihilation spectroscopy (PAS) may be possible under the existence of a positron flux (Eq. 1), an effective interaction of positrons with matter along the entire periphery of the active nuclei of galaxies, and the presence of radiation responses in their γ and optical spectra. All these conditions can be satisfied in AGNs, for example, in BL Lac type objects.

At the final stages of the first and second cascades of interest, positrons with energies within the range of 0.1–5 MeV are formed. The semi-empirical electron and positron energy distribution function $\varphi_{e\pm}$, reported by Gusev et al. (2000), is particularly worthy of notice. It uses the same form for electrons and positrons; furthermore, at $E_0 = 2$ GeV, it can be expressed by the following formula:

$$\varphi_{e\pm} \approx (E/E_0)^{3.045 \pm 0.080}$$

According to the electron energy distribution function, f(E), the resulting electron energy distribution, F(E), in the left low-energy portion is mathematically represented as $F(E) = f(E) + \varphi_{e^-}$. This indicates that left low-energy portion F(E) represents a local maximum that reflects the yield of Auger electrons. Therefore, energy losses due to ionization, along with the results of triggered cascades (1), lead to a noticeable increase in the proportion of electrons created, and thus, contribute to the soft X-ray and hard ultraviolet emission within the bulk of the AGN.

The aforementioned mechanism of mechanical energy transfer to gas-and-dust aggregates via energy loss due to ionization does not imply the induction of stimulated emission in the soft γ-ray band as pointed by Doikov et al. (2018). On the other hand, it proves to be an efficient means of maintaining high luminosity of the AGN in the optical,

ultraviolet, and soft X-ray bands.

2. THE POSITRON ANNIHILATION: SINGLE-PHOTON ANNIHILATION OF POSITRONS

Dermer (1997) and Jung (1996, 1998) investigated the deceleration of incident positrons to states at which their energies became comparable to those of the average binding energies of the K-shell electrons of the target atoms. When annihilation occurs, a vacancy (or a hole) is created at the associated energy level; a single γ-quantum is emitted with the residual momentum being transferred to the atomic nucleus. Our earlier studies (Doikov et al. 2018, 2019) focused on the solution of this problem. In particular, we solved the set of equations given below using the laws of conservation of energy and momentum:

$$E_p + 2m_e c^2 = E_\gamma + E_n + E_b \quad (2)$$

$$P_p = P_\gamma + P_n \quad (3)$$

In these equations, E_p, P_p, E_n, P_n, E_γ, and P_γ are the energies and momenta of the incident positron, recoiling nucleus, and emitted γ-quantum, respectively, and E_b is the binding energy of the K-shell electron. Cross-sections of the presented reaction were obtained by applying the techniques of quantum electrodynamics, using the formulae selected and reported by Mikhailov & Mikhailov (1998) and Mikhailov et al. (2013).

In the range of energies considered here, we postulated a non-relativistic approximation for the positron flux. The set problem was solved using the Hartree units ($m_e c^2 = 1$, $h = c = m_e = 1$, $P = \sqrt{2mE}$) and on squaring equation (3), we obtained the following:

$$E_p + 2 = E_\gamma + E_n + E_b \quad (4)$$

$$2E_p = E_\gamma^2 + 2 \lfloor E_\gamma \rfloor \sqrt{2m_n E_n} \cos\alpha + 2m_n E_n \quad (5)$$

We assume that the order of smallness for the scattering angles at the investigated energies is cosα ≈ 1. A solution for the given set of equations, based numerical methods, has been discussed by Doikov (2018) wherein it has been proved that a failure to fulfill the small-angle scattering assumption yields physically incorrect resulting energy E_γ of the γ-quantum generated by annihilation with a K-shell electron.

This fact is consistent with results from experiments on the scattering of fast particles, whose de Broglie wavelength

was comparable to that of the geometric scales of K-shells of target atoms as shown by Doikov et al. (2018). Based on the solution found for the set of equations (4) and (5) at different values of spectroscopic parameters of atoms, we obtained a relationship between E_γ and E_n, which was the ultimate goal of positron annihilation spectroscopy.

In this paper, we proceed with the calculations commenced in our previous study (Doikov et al. 2019) for the following elements - $_2^3$He, $_3^6$Li, $_3^7$Li, $_4^7$Be, $_4^9$Be, $_5^{10}$B, and $_5^{11}$B . The values of E_γ and E_n, obtained for these elements, enable us to relate the single-photon annihilation of each element to the Doppler broadening of their respective optical lines. Table 1 presents an extended set of data that allows us to estimate the Doppler broadening of spectral lines with a hypothetical zero-point taken to be at the wavelength of 4,000 Å.

The diffusive pattern of interstellar medium surrounding the AGN implies the presence of hyperfine diffuse series of spectral lines that are typical of gaseous nebulae. In this case, the Doppler broadening of spectral lines in the optical band will be equal to $\Delta\lambda_D = \lambda(v/c)$, where λ is the wavelength of the emission lines produced by unexcited atoms; v is the recoiling nucleus velocity, and **c** is the speed of light in vacuum.

In Table 1, we have also provided the Doppler broadenings, $\Delta\lambda_D$, for different isotopes of the chemical elements investigated here at a wavelength of 4,000 Å. Line broadenings of this order can be measured using modern spectroscopic methods.

Dynamical and spectroscopic characteristics presented in Table 1, along with the cross-section of single-photon annihilation, enabled us to draw conclusions about the availability and efficiency of the **positron annihilation spectroscopy** method to study the AGN. The rate of γ-quanta production during single-photon annihilation is defined by the cross-section of the process represented in Table 1 as the

common logarithm, lg $\sigma_{e^+}^+$. This allowed us to estimate the resulting number of single-photon electron-positron annihilation events in a gas by using the number density n and layer thickness Δr. This number is equal to N = σ_{e^+}n∆r .

The second important finding is the dependence of the γ-quantum energy E_γ on the incident positron energy E_p and K-shell electron binding energy E_b. When E_p is close to E_b, the energies of the γ-quanta generated, E_γ, are weakly sensitive to E_p.

This fact gives grounds for the interpretation of the blurring of such emission lines as sensitivity to the function f(E). Therefore, the structure of the emission lines, E_γ, produced by single-photon annihilation is governed by the total impact of the positron energy distribution, f(E), and the cross-section of positron annihilation with atomic K-shell electron, $\sigma_{e^+}^+$.

3. DISCUSSION

According to quantum electrodynamics, annihilation yields spectral lines at 0.511 and 1.022 MeV in the γ-ray band. This paper shows that single-photon annihilation results in the Doppler broadening of spectral lines due to the transitions of electron for the elements, which gained the recoil momentum. Table 1 presents the wavelengths of spectral lines of the respective elements and Doppler broadening for these lines.

These lines are sufficiently thin in the diffuse medium of AGN; hence, their Doppler broadening should be noticeable. The profiles of γ-lines were determined by the contribution of each element that experienced the single-photon annihilation at energies close to E_γ = 1.022 MeV, thus producing the visual effect of blurring the sharpness of each emission line. This phenomenon is associated with

Table 1. The dynamic and spectroscopic characteristics of light elements involved in single-photon annihilation processes

Chemical elements	Atomic mass	E_b (eV)	lg $\sigma_{e^+}^+$	E_γ (MeV)	E_n (MeV)	$\Delta\lambda_D$ (Å)
$_1^1$H	1.0081	13.602	−26.8551	1.026533	0.000564	3.121882
$_1^2$H	2.0141	13.602	−26.8551	1.026629	0.000467	2.01515
$_2^3$He	3.0160	24.586	−25.6339	1.026818	0.000267	1.242655
$_2^4$He	4.0026	24.588	−25.6340	1.026873	0.000213	0.962207
$_3^6$Li	6.0151	64.400	−25.2194	1.026932	0.000114	0.573492
$_3^7$Li	7.0160	64.400	−25.2194	1.026912	0.000134	0.575918
$_4^7$Be	7.0169	123,600	−24.9133	1.026908	7.84E-05	0.448658
$_4^9$Be	9.0122	123,600	−24.9133	1.026908	7.84E-05	0.389221
$_5^{10}$B	10.013	201.000	−24.6685	1.026852	0.000111	0.314402
$_5^{11}$B	11.009	201.000	−24.6685	1.026896	2.61E-05	0.145201

Atomic mass is expressed in atomic mass units; E_b is the K-shell electron binding energy; lg$\sigma_{e^+}^+$ is the common logarithm of the cross-section for the interaction of the positron $\sigma_{e^+}^+$(cm^2); Eγ(MeV) is the energy of γ-quanta generated by annihilation; E_n (MeV) is the recoiling energy of light atomic nuclei after annihilation; and $\Delta\lambda_D$ (Å) is the Doppler broadening of spectral line with a hypothetical zero-point at the wavelength λ=4,000 Å.

a non-linear relationship between the values of E_γ and E_n in equations (4) and (5). The effect is leveled out when the majority of atoms in the investigated environment are represented by a small number of chemical elements, for instance, by only light chemical elements. This is the case for the AGN.

Young supernova remnants contain a large variety of different chemical elements including radioactive isotopes. Some radioactive decays are accompanied by γ-quanta emissions at their respective frequencies. In particular, a radioactive series such as $^{44}_{22}Ti \xrightarrow{85y} {}^{44}_{21}Sc \xrightarrow{6h} {}^{44}_{20}Ca$ in supernova remnants results in the emission of γ-quanta with the energy E_r = 1.217 MeV. Such processes should be employed, with caution, to interpret the γ-spectra in the AGN, as noted earlier by Dermer (1997).

When the optical spectra are generated in relatively stationary regions of the AGN, a noticeable Doppler broadening, represented in the last column of Table 1, occurs in the optical lines of rare-earth elements, along with the single-photon annihilation processes in target atoms and double-photon annihilation in dust grains. This creates new opportunities for investigation of the profiles of respective lines and for interpretation of physical processes. During the last decade, γ-spectra of distant AGN and supernova remnants have been obtained with an accuracy of several KeV (Fan et al. 2016).

In the case presented in this report, γ-ray lines can be classified by their origin:

- Lines generated in nuclear radioactive transitions (β-decays) with energies ranging from a few tens of KeV to 10 MeV;
- Lines produced by the annihilation of positrons with electrons (with energies of 0.511, 1.022 MeV);
- Lines resulting from the collision of heavy cosmic rays with respective target atoms (spallation reactions).

The dynamical and spectroscopic characteristics presented in Table 1, along with the cross-section of single-photon annihilation, enable us to draw conclusions about the availability and efficiency of a PAS method for studying the AGN.

4. CONCLUSIONS

This paper considers the main reaction channels that result in the formation of positrons. The overabundance of positrons compared to their background content provides information on the processes that resulted in their formation. However, single- and double-photon annihilation should occur when positrons undergo sufficient

deceleration. In this case, γ-quanta with energies of 0.511 MeV and 1.022 MeV are generated as the radiative feedback of the medium.

Intense collisions of protons and high-energy α-particles (up to 2 GeV) that form a massive component of cosmic rays should be considered to be a two-channel source of positrons in the AGN. The first channel is described by formulae (1). The second source is associated with the cosmic rays involved in spallation reactions, resulting in the evaporation of neutrons of the target atoms with atomic masses of up to 58 amu.

In this case, provided that there were no other sources of fast electrons, non-thermal luminosity of the medium within the range of energies up to 10 KeV was dominated by the losses of energy due to ionization by fast positrons (80% of the total non-thermal luminosity) and, to a lesser extent, by fast electrons (15%–20%). The results of calculations obtained in this study, as well an earlier study by Doikov (2018) and Doikov et al. (2019), showed that one can expect an increase of five orders of magnitude in the rate of positron production in the entire bulk of the active region of the AGN.

As a result of positron annihilation, the integrated brightness of the peripheral regions will be observed in γ-lines with energies of 0.511 MeV and 1.022 MeV generated by annihilation of positrons with a maximal proportion of their energy distribution function f (E) being localized at $E_p \approx 0.01\ MeV$. During annihilation of positrons with the K-shell electrons, the nuclei of target atoms gain recoil momentum. Only these nuclei exhibit Doppler broadening of their optical lines in the AGN, which makes it possible for them to improve diagnostic capabilities for observations of the diffuse component of such objects.

REFERENCES

Crosas M, Weisheit J, Spallation in active galactic nuclei, Astrophys. J. 465, 659-665 (1996). http://doi.org/10.1086/177451

Dermer CD, The production spectrum of a relativistic Maxwell-Boltzmann gas, Astrophys. J. 280, 328-333 (1984) http://doi.org/10.1086/161999

Dermer CD, Binary collision rates of relativistic thermal plasmas. II Spectra, Astrophys. J. 307, 47-59 (1986). http://doi.org/10.1086/164391

Dermer CD, Skibo JG, Annihilation fountain in the galactic center region, Astrophys. J. 487, L57-L60 (1997). http://doi.org/10.1086/310870

Doikov DN, Positron annihilation spectroscopy of young supernova remnants, Odessa Astron. Publ. 31, 62-69 (2018),

http://doi.org/10.18524/1810-4215.2018.31.144437

Doikov DN, Andrievsky SM, Yushchenko AV, Gas and dust emission in cold environment with enhanced content of radioactive $^{44}_{22}Ti$ isotope, J. Phys. Stud. 22, 2901 (2018). https://doi.org/10.30970/jps.22.2901

Doikov DN, Yushchenko AV, Jeong Y, Positron annihilation spectroscopy of active galactic nuclei, J. Astron. Space Sci. 36, 21-33 (2019). http://doi.org/10.5140/JASS.2019.36.1.21

Fan JH, Yang JH, Liu Y, Luo GY, Lin C, et al., The spectral energy distributions of Fermi Blazars, Astrophys. J. Suppl. Ser. 226, 20 (2016). http://doi.org/10.3847/0067-0049/226/2/20

Gusev AA, Jayanthi UB, Martin IM, Pugacheva GI, Spjeldik WN, On positron radiation belt in the Earth's magnetosphere, Braz. J. Phys. 30, 590-593 (2000). http://doi.org/10.1590/S0103-97332000000300017

Jung YD, One-photon annihilation of nonthermal positrons in the interstellar medium, Astrophys. J. 457, 431-434 (1996) http://doi.org/10.1086/176742

Jung YD, One-photon annihilation of thermal positrons in the interstellar medium, Astrophys. J. 500, 1055-1058 (1998) http://doi.org/10.1086/305749

Mikhailov AI, Mikhailov IA, Annihilation of a relativistic positron and K-electron to yield a photon and second K-electron, J. Exp. Theor. Phys. 86, 429-438 (1998). https://doi.org/10.1134/1.558515

Mikhailov AI, Mikhailov IA, Nefiodov AV, Plunien G, Excitation of autoionizing states of helium-like ions by scattering of high-energy particles, J. Exp. Theor. Phys. 116, 363-371 (2013). https://doi.org/10.1134/S1063776113020155

Moskalenko IV, Strong AW, Production and propagation of cosmic-ray positrons and electrons, Astrophys. J. 493, 694-707 (1998), https://doi.org/10.1086/305889